Scientific Research Publishing

Open Journal of Modern Hydrology, 2022, 12, 55-73
https://www.scirp.org/journal/ojmh
ISSN Online: 2163-0496
ISSN Print: 2163-0461

Hydrometeorological Modeling of Limpopo River Basin in Mozambique with TOPMODEL and Remote Sensing

Tomásio Eduardo Januário[1], Augusto José Pereira Filho[1], Marcos Figueiredo Salviano[2]

[1]Department of Atmospheric Sciences, Institute of Astronomy, Geophysics and Atmospheric Sciences, University of São Paulo, São Paulo, Brazil
[2]Geological Survey of Brazil, São Paulo, Brazil
Email: tomasio.januario@usp.br, augusto.pereira@iag.usp.br, marcos.salviano@cprm.gov.br

How to cite this paper: Januário, T.E., Pereira Filho, A.J. and Salviano, M.F. (2022) Hydrometeorological Modeling of Limpopo River Basin in Mozambique with TOPMODEL and Remote Sensing. *Open Journal of Modern Hydrology*, **12**, 55-73.
https://doi.org/10.4236/ojmh.2022.122004

Received: February 15, 2022
Accepted: April 8, 2022
Published: April 11, 2022

Abstract

The Limpopo River basin (LRB) is known for its vulnerability to floods, high rates of evapotranspiration, and droughts that cause significant losses to the local community. The present study aimed to perform simulations of flood events occurring in two Mozambican sub-basins of LRB, namely *Chókwè* and *Xai-Xai* from 2000 to 2015 with TOPography-based hydrological MODEL (TOPMODEL) and satellite remote sensing data. As input in TOPMODEL, data from two high-resolution global satellite-based precipitation products: Climate Prediction Center MORPHing technique (CMORPH) and Integrated Multi-Satellite Retrievals for the Global Precipitation Mission (GPM) algorithm (IMERG), 8-day MOD16 evapotranspiration product and surface runoff data estimated by Global Land Data Assimilation System (GLDAS) were used. The sensitivity tests of TOPMODEL parameters were applied using the Monte Carlo simulation. Calibration and validation of the model were performed by the Shuffled Complex Evolution (SCE-UA) method and were evaluated with the Kling-Gupta Efficiency (KGE) index. The results indicated that simulations with the GPM-IMERG (KGE: 0.59 and 0.65) tended to underestimate the stream flows, while with the CMORPH product the performance was much better (KGE: 0.66 and 0.77) in both sub-basins. Thus, TOPMODEL can help to develop flood monitoring systems from satellite remotely sensed data in similar regions of Mozambique.

Keywords

Floods Simulations, Limpopo River, TOPMODEL, CMORPH, IMERG

1. Introduction

Mozambique is a developing country, with a climate predominantly humid to semi-humid, and in the estuary of several rivers, sharing nine (9) of the fifteen (15) international river basins in the Southern African Development Community (SADC) [1] [2]. Due to these conditions, the country is extremely vulnerable to extreme weather events such as floods, cyclones, droughts, and other events, which tend to turn into calamities. Population growth and urbanization processes, in line with land use trends, the increasing impoverishment of the population, the uncontrolled use of technological systems, and inadequate sanitation systems, among others, are the factors that increase the vulnerability of the population to such extreme weather events [3] [4] [5] [6].

A flood is a natural phenomenon with great destructive power that happens quickly and sometimes unexpectedly. It forms when intense rainfall causes an increase in the flow of water channels, which results in a rise in water levels and consequent leakage of the banks [7] [8]. The impacts of floods range from deaths, destruction of many types of infrastructures, the spread of diseases, and interdiction of roads. In the year 2000, floods associated with several cyclones had a particular impact on the lives of Mozambican populations [1] [9]. The LRB, with a total catchment area of approximately 411,000 km^2, is known for its vulnerability to floods, high rates of evapotranspiration, and droughts that cause significant losses to the local community [8] [10]. Floods are the biggest problem in the LRB, particularly in the low-elevation areas across the coastal floodplain in Mozambique, a region that receives a large portion of the water from the upper basin [3] [6] [7] [8] [11] [12]. According to [13] a better understanding of the nature of rainfall extremes on the LRB is crucial for decision-makers, disaster managers, and seasonal forecasts of wet or dry seasons and in evaluating how the regional water cycle may behave in the future climate. However, as an alternative, hydrological models have been used [14].

TOPMODEL, developed by Beven & Kirkby in 1979 [15], is classified as a semi-distributed and conceptual rainfall-runoff hydrological model based on the variable contribution area and has been the subject of numerous applications to a wide variety of catchments [15] [16] [17]. Parameters in the model are intended to be physically interpretable and their number is kept to a minimum to ensure that values determined by a calibration exercise should be more easily identifiable, while still allowing mapping of the predictions back into the catchment based on the pattern of a topographic index derived from an analysis of flow paths in the catchment [18] [19].

Accurate rainfall measurements are required, usually over broad areas because of the natural variability of rain. Coverage of a large area can be achieved using many distributed point measurement techniques (e.g. rain gauges) or using remote sensing (radars and satellites) to estimate rainfall over such an area [20]. The latest satellite-based precipitation products measure precipitation with very high spatial and temporal resolutions. To achieve those resolutions, they combine infrared (IR) images with passive microwave (PMW) echoes to produce precipitation estimates [21]. Two multi-satellite sensor precipitation products are used in this study: the Climate Prediction Center (CPC) MORPHing technique (CMORPH) [22] of US National Oceanic and Atmospheric Administration (NOAA) and the Integrated Multi-Satellite Retrievals (IMERG) [23] for the Global Precipitation Mission (GPM) of US National Aeronautics and Space Administration (NASA). Potential evapotranspiration (PET) data from the Moderate Resolution Imaging Spectroradiometer (MODIS) algorithm for Global Evapotranspiration Project (MOD16) [24] and surface runoff data from the Global Land Data Assimilation System (GLDAS) [25] were also used in this study.

The performance of conceptual rain-runoff (CRR) models depends on the adequacy of the estimation of their parameters (calibration). Hence, the model must be able to identify appropriate values for its parameters [26] [27]. Model performance criteria are often used during calibration and evaluation processes. Traditionally, the Nash-Sutcliffe efficiency (NSE) [28] is an often-used metric to summarize model performance. Increasingly an alternative metric, the Kling-Gupta efficiency (KGE), is used instead [29] [30]. Research on automatic calibration methods in the search for optimal parameter sets in CRR models has led to the development of several methods [18] [26] [31] [32] [33]. A global optimization method known as the SCE-UA (Shuffled Complex Evolution method developed at the University of Arizona) has shown promise as an effective and efficient optimization technique for calibrating CRR models [31]. The use of interactive techniques to optimize the parameters of a model must be preceded by a study of sensitivity analysis and the importance of these model's parameters [33] [34].

Thus, this study aims to perform simulations of flood events occurring in two Mozambican sub-basins of LRB, namely *Chókwè* and *Xai-Xai,* from 2000 to 2015 with TOPMODEL and satellite remote sensing data as input. In Section 2, a brief description of the study area is presented. Then, is described the TOPMODEL hydrological model, used to perform simulations in both sub-basins. Different datasets derived from satellite-based techniques used to estimate precipitation, estimate surface runoff, and PET, are also described. Data from the Digital Elevation Model (DEM) from the SRTM mission (resolution ~90 m) were used to calculate the topographic index of the basin, TOPMODEL's basic input for streamflow simulation. The calibration and validation of the model were performed by the SCE-UA method and were evaluated with the Kling-Gupta Efficiency (KGE) metric. The results of applications of those methods are presented and discussed in Section 3, followed by the conclusions and recommendations in Section 4.

2. Material and Methods

2.1. Study Area

The Limpopo River has a 411,000 km^2 drainage area and is ~1760 km long with its outlet at the Indian Ocean (**Figure 1**). It is located between latitudes 20˚S - 26˚S and longitudes 25˚E - 35˚E distributed in four riparian countries, South Africa (45%), Botswana (19%), Zimbabwe (15%) and Mozambique (21%) [10]

[11]. The LRB is one of the 63 transboundary basins in Africa and the fourth largest in southern Africa, smaller than Congo, Zambezi, and Orange basins [7] [8] [9] [13].

This study focuses on two sub-basins where hydrological simulations were performed, namely, *Chókwè* and *Xai-Xai*, all of them with an outlet in Mozambique (**Figure 2**). By Thornthwaite's criterion, the climate of the Mozambican part of the basin varies from arid (E) near the border, semi-arid (D) in the central region, and sub-humid dry mega thermal (C1) in the lower part of the basin [1] [10] [11].

In the basin, the temperature is strongly related to the topography. The annual average in the Mozambican part ranges from 23˚C to 26˚C. Precipitation is highly seasonal and unevenly spatially distributed, with an annual average of 530 mm, ranging from 400 mm in the hot and dry areas of the west and central to 1600 mm in the central-southern fraction. Precipitation occurs mainly in the summer (October to March), with January the wettest month [6] [9]. Evaporation ranges from 1700 to 2300 mm, a higher rate than precipitation. The average annual relative humidity varies between 65 and 70%. The high rates of evapotranspiration mean that most of the rain does not contribute to river flow or groundwater recharge [6] [9] [13]. The most important meteorological systems that determine precipitation volumes and patterns in LRB are the Inter-tropical Convergence Zone (ITCZ); Tropical-Temperate-Troughs (TTTs); cold fronts [6], and the tropical systems (cyclones, depressions, storms) of the South Western Indian Ocean (SWIO) [1] [2] [4] [12] [35].

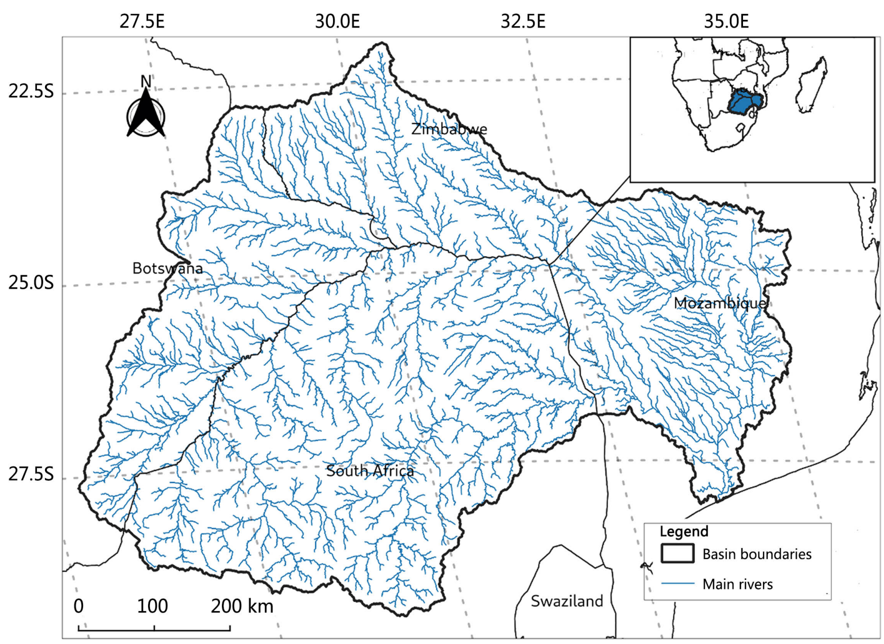

Figure 1. Map of the Limpopo River Basin in southern Africa with riparian countries. As indicated in the figure: basin boundaries (thick black line), main rivers (thin blue lines), a distance scale (km), geographic contours (light black). Longitudes are plotted on the x-axis and latitudes on the y-axis.

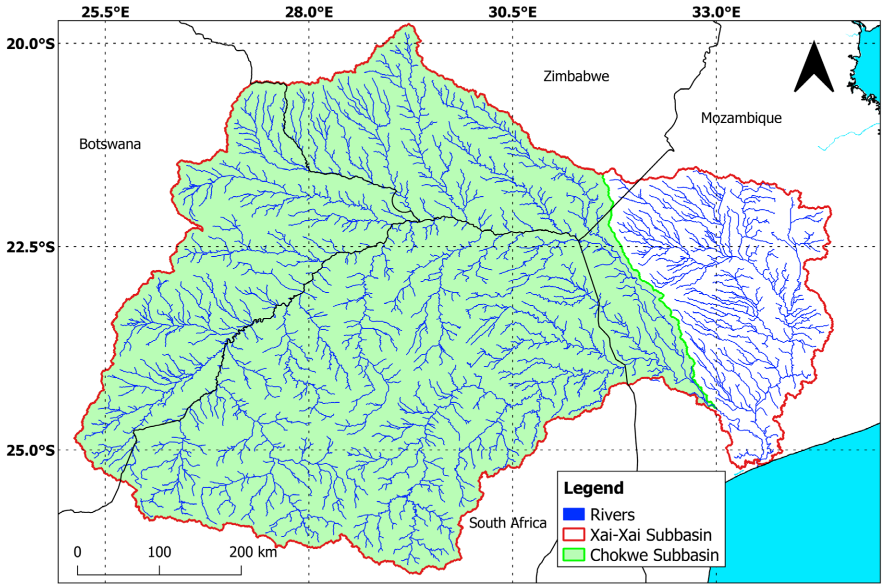

Figure 2. Delineation of Mozambican sub-basins in LRB. Geographic boundaries, main rivers (thin blue lines), distance scale (km), *Xai-Xai* sub-basin (red outline), and *Chókwè* sub-basin (green fill) are represented. Longitudes are plotted on the x-axis and latitudes on the y-axis.

2.2. Database

The database employed in this study includes two satellite-based precipitation estimates products: Climate Prediction Center MORPHing technique (CMORPH) [22] and Integrated Multi-Satellite Retrievals for the Global Precipitation Mission (GPM) algorithm (IMERG) [23]. Satellite-based potential evapotranspiration estimation from the Moderate Resolution Imaging Spectroradiometer (MODIS) algorithm for Global Evapotranspiration Project (MOD16) algorithm [24] and surface runoff data from the Catchment Land Surface Model (CLSM/GLDAS) model [25] are also used. A summary of the databases used is presented in Table 1.

2.2.1. Precipitation

GPM is a collaborative mission between the National Aeronautics Space Administration (NASA) and the Japan Aerospace Exploration Agency (JAXA). The two main GPM satellite sensors are the DPR and GMI, both derived from the acronyms Dual-Frequency Precipitation Radar and the GPM Microwave Imager. The GMI (active sensor) is used to estimate the type and intensity of the precipitation, while the DPR (passive sensor) is used to explore the internal structure of the storms under or within clouds [23] [36]. TRMM and GPM satellites were used to produce multi-satellite products, such as TMPA and IMERG. Input precipitation estimates calculated from the various passive satellite microwave sensors are inter-calibrated to the GPM Combined Instrument product, then "transformed" and combined with geo-IR fields calibrated by microwave precipitation, and fitted with precipitation data monthly surface meters (when available) to provide precipitation estimates. The precipitation phase is diagnosed using

Table 1. List of remote sensing products used. First column: product name. Second column: estimated variable. Third column: spatial and temporal resolution. Fourth column: product references.

Product	Variable	Resolution	Reference
GPM IMERG Final	Precipitation	0.1˚ - 30 min	[23]
CMORPH_V1.0	Precipitation	8 km - 24 h	[22]
MOD16	Potential Evapotranspiration	500 m - 8 day	[24]
GLDAS-2.0, GLDAS-2.2	Surface runoff	(0.25˚, 1.0˚), (3 h, 24 h)	[25]

temperature, humidity, and surface pressure analyses. In this study, data from the final execution of the IMERG (IMERG_F version 6) were used, with a spatial resolution of 0.1˚ and temporal resolution of 30 minutes, for the period of 2 March 2003 to February 22, 2015. The database was available at https://disc.gsfc.nasa.gov/datasets/.

The CMORPH is a technique that produces global precipitation estimates from PMW and IV data at high spatial resolution (approximately 8 km on the line of the equator) and temporal (30 minutes) [22]. Precipitation rates are obtained from PMW from low orbit satellites and advected by winds derived from IR measurements from geostationary satellites. The CMORPH technique uses different satellite sensors to produce the best possible precipitation estimate [37] [38]. The result of this process is a spatial interpolated precipitation field temporally generated by microwaves with high spatial and temporal resolution [39]. The results from several authors on the errors inherent in this rainfall estimate are satisfactory and allow for a more detailed analysis of tropical dynamics, especially where the surface observations are scarce [22] as is the case in the LRB region. The CMORPH_V1.0 product with 8km spatial resolution and temporal resolution 24 hours, selected for this study, is available at https://www.ncei.noaa.gov/access/metadata/landing-page/.

2.2.2. Potential Evapotranspiration

The Moderate Resolution Imaging Spectroradiometer (MODIS) for Global Evapotranspiration Project (MOD16) is a global ET estimation algorithm proposed for the first time by Mu *et al.* (2011) [24]. The algorithm (MOD16) is based on the logic of the Penman-Monteith equation which uses daily meteorological reanalysis data as inputs (incident solar radiation, average air temperature, average air temperature during the day, minimum air temperature, and water vapor pressure) and remote sensing data from the MODIS database such as land use and land cover MCD12Q1, vegetation index MOD13Q, leaf area index LAI/FPAR MOD15A2 and albedo MOD43C1 at the spatial resolution of 0.05˚ [40] [41] [42]. The MOD16 dataset covers 109.03 million km^2 of vegetation areas globally and is designed by the MODIS sensor onboard the Aqua and Terra platforms, with registration data from 2000 to the present day. The MOD16A2 Potential Evapotranspiration data was used in this study set of 500 meters of spatial resolution and accumulated values of 8-days in sinusoidal projection

(MODIS/Terra Net Evapotranspiration Gap-Filled 8-Day L4 Global 500 m SIN Grid V006), for the period from January 18, 2000, to February 22, 2015. The data of MOD16A2 are provided by the NASA server (https://lpdaacsvc.cr.usgs.gov/).

2.2.3. Surface Runoff

The GLDAS [25] was developed through a partnership between the Goddard Space Flight Center (GSFC) of NASA and NOAA's National Centers for Environmental Prediction (NCEP) to produce a new generation of spatial and surface-measured climate data [43]. GLDAS is a global model that uses advanced data modeling techniques for Earth surface and data assimilation to provide high spatial resolution reanalysis (0.25˚ to 1 km) from meteorological stations distributed all over the planet and data from meteorological satellites. The data was acquired as part of the Earth Science Division Mission, archived and distributed by Goddard Earth Sciences (GES) Data and Information Services Center (DISC). Data from the Catchment Land Surface Model (CLSM) were used.

Two components of NASA's GLDAS Version 2 (GLDAS-2) were used: GLDAS-2.0, and GLDAS-2.2. The main purpose of GLDAS-2.0 is to create climatologically consistent datasets using data from the Global Meteorological Forcing Dataset from Princeton University, covering 1948 to 2014. The GLDAS-2.2 component dataset uses data assimilation, while the products GLDAS-2.0 and GLDAS-2.1 are "open loop" (*i.e.*, no data assimilation). Time resolutions for GLDAS-2 products are three hours and daily, with spatial resolution of 0.25˚ and 1.0˚. In this study, two streamflow outputs (Q_S and Q_{Sb}) of the component were used. GLDAS-2.0 (period from January 18th to March 28th, 2000) and GLDAS-2.2 (period from 2nd of March 2003 to February 22, 2015), were available at: https://disc.gsfc.nasa.gov/datasets. Data from the 3 variables were processed, namely: Q_S, Q_{Sb} and $Q_{\text{total}} = Q_S + Q_{Sb}$. In theory, the sum of these two variables of flow corresponds to the flow generated by each point (pixel). The data obtained for Q_{Sb} was of only zero value for most of the selected period. Thus, the calibration of the TOPMODEL [15] was performed with only Q_S data, since in outputs of TOPMODEL, there is a separation of the streamflow (surface flow of the GLDAS and Runoff simulated by TOPMODEL).

2.3. TOPMODEL

According to Beven *et al.* (1984) [16] the physically-based computer model of basin hydrology presented here (called TOPMODEL from TOPography-based hydrological MODEL), was formulated by [15]. The TOPMODEL is a variable contributing area conceptual model. Although conceptual, this model is frequently described as a physically-based model in the sense that its parameters can be measured directly *in situ* [32]. It is premised upon two basic assumptions that: the dynamics of the saturated zone can be approximated by steady-state representations of the saturated zone on an area draining to a point on a hillslope and that the hydraulic gradient of the saturated zone can be approximated by the local surface topographic slope, $\tan\beta$ [18]. These assumptions lead to simple relationships between catchment storage (or storage deficit below saturation) in which the main factor is the Kirkby topographic index (λ), the only spatially distributed parameter [Equation (1)] [44]. The λ represents the propensity of any point in the catchment to develop saturated conditions [18].

$$\lambda_i = \ln\left(a_i / T_0 \tan\beta_i\right) \tag{1}$$

where λ_i is topographic index class; a_i is the area of the hillslope per unit contour length [m²] that drains through point i; T_0 is local saturated transmissivity [$m^2 \cdot h^{-1}$] and $\tan\beta_i$ is local surface topographic slope [$m \cdot m^{-1}$].

TOPMODEL is based on the storage principle of Darcy flow equation [18] [32] [45] and consists of a series of interconnected reservoirs with different times constant (**Figure 3**). The distribution of downslope transmissivity T_0 with depth can be simulated by an exponential function, Equation (2):

$$T_i = T_0 e^{-D_i/m} \tag{2}$$

where T_i is transmissivity at point i [$m^2 \cdot h^{-1}$] and m is decay of transmissivity with depth; D_i is the local saturation deficit. The m parameter acts as a controller of the effective depth of the soil profile and, together with T_0, determines the active zone of the soil where subsurface runoff occurs [45] [46].

The series of reservoirs in TOPMODEL represents the mean soil saturation response in a homogeneous sub-basin. The dominant source in the generation of runoff (Q) is rain (R). Part of the net precipitation can be lost by evapotranspiration in the root zone storage (S_{RZ}) and another part in the gravity drainage zone storage (S_{UZ}) [18] [32]. Actual evapotranspiration (ET_a) losses, are controlled by potential evapotranspiration (ET_p) and the maximum root zone storage ($S_{r\max}$) [47]. The topography of a catchment is analyzed using Digital Elevation Model (DEM) data through a Geographic Information System (GIS). The DEM data from the Shuttle Radar Topography Mission (SRTM, approximately 90 m resolution) was used to generate the spatial distribution of λ [16] [32] [45] [48]. From the λ values the distribution relative to the percentage of area in the *basin* is obtained, which is the basic input of TOPMODEL to simulate the streamflow of the basin [46].

2.4. Calibration and Validation Evaluation

To calibrate TOPMODEL's parameters the Shuffled Complex Evolution (SCE-UA) method was used. The SCE-UA method was developed at the University of Arizona and is a global optimization algorithm, initially developed by Duan *et al.* (1992) [26] for the calibration of CRR models. SCE-UA searches for the global optimum of a function by evolving clusters of samples drawn from the parameter space, via a systematic competitive evolutionary process [27].

The calibration and validations were evaluated through Kling-Gupta efficiency metric (KGE) [29]. The KGE, Equation (3), is based on a decomposition of NSE [Equation (4)] into its constitutive components (correlation, variability bias, and mean bias), addresses several perceived shortcomings in NSE, and is increasingly used for the CRR model calibration and evaluation:

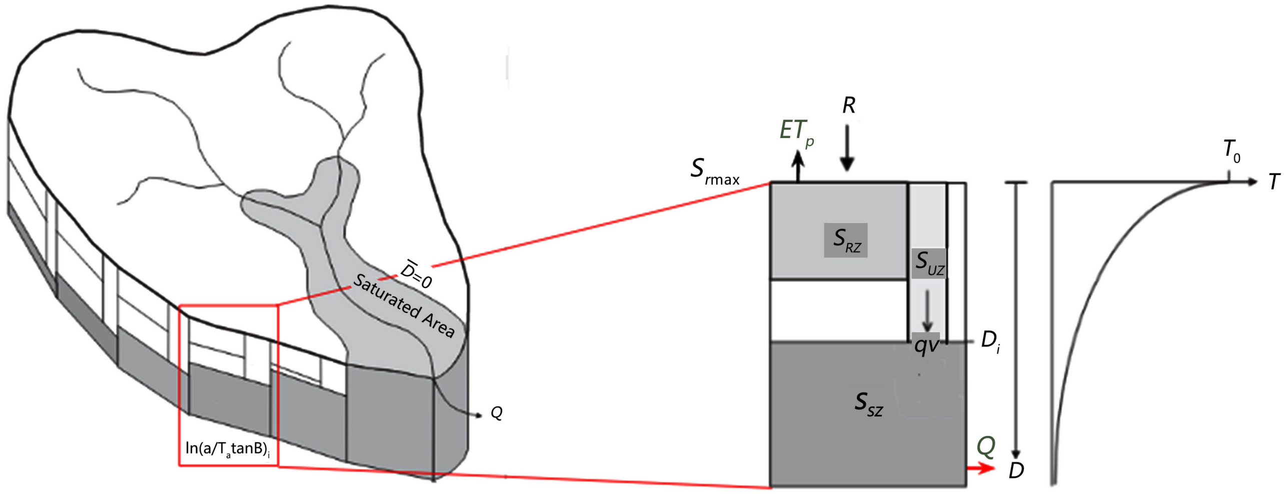

Figure 3. Schematic diagram of prediction of saturated area using increments of the topographic index distribution in TOPMODEL. Where $\underline{D}$ —mean saturation deficit; Q—subsurface flow; R—effective recharge rate; ET_p—potential evapotranspiration; S_{RZ}—root zone storage; $S_{r\max}$—Maximum root zone storage deficit; S_{UZ}—unsaturated zone storage; S_{SZ}—saturated zone storage; D_i—local saturation deficit; D—water table depth; T_0—local saturated transmissivity and T—transmissivity of saturated surface soil layer. Adapted from [18].

$$\text{KGE} = 1 - \sqrt{(r-1)^2 + \left(\frac{\sigma_{sim}}{\sigma_{obs}} - 1\right)^2 + \left(\frac{\mu_{sim}}{\mu_{obs}} - 1\right)^2} \tag{3}$$

$$\text{NSE} = 1 - \frac{\sum_{t=1}^{n}\left(Q_{sim}^{t} - Q_{obs}^{t}\right)^2}{\sum_{t=1}^{n}\left(Q_{obs}^{t} - \overline{Q_{obs}}\right)^2} \tag{4}$$

where r is the correlation between observed and simulated values; σ represents the standard deviation; μ represents a time series average; n is the number of time steps; t is the time step in days; Q_{sim} is the simulated value; Q_{obs} is the observed value; and $\overline{Q_{obs}}$ is average streamflow observed. Like NSE, KGE = 1 indicates perfect agreement between simulations and observations; KGE > 0 is indicative of "good" model simulations, whereas KGE < 0 are considered "bad"; KGE = 0 indicates threshold between "good" and "bad" performance [29] [30].

3. Results and Discussions

In this current section, we present and discuss the results of our analysis obtained using the R statistical programming packages and Q-GIS. Five flood events that occurred in the two Mozambican sub-basins, namely, *Chókwé* and *Xai-Xai* basins between 2000 and 2015 were chosen to carry out simulations with the TOPography-based hydrological MODEL (TOPMODEL). The first event (Event 1) selected, took place between January 18 and March 28 of 2000 (71 days of duration); the second one (Event 2), lasting 26 days, occurred between March 2nd and 27th, 2003; the third (Event 3) from December 7, 2011, to March 29, 2012 (85 days); the fourth (Event 4) took place from January 10 to February 14, 2013 (36 days duration); the fifth (Event 5) and last (71 days of duration) took place between December 14, 2014, to February 22, 2015. The selection of flood events was based on the preliminary analysis of the hydrometric data series provided by the National Directorate of Water Resources Management of Mozambique (DNGRH), which is the authority responsible for water management.

In Section 3.1, the results of the application of the Monte Carlo simulations are presented, with both precipitation datasets: Climate Prediction Center MORPHing technique (CMORPH) and Integrated Multi-Satellite Retrievals for the Global Precipitation Mission (GPM) algorithm (IMERG). The MC method was used to generate the TOPMODEL's parameter values randomly in the sub-basins, with 5000 iterations for each flood event. Calibration and validation of TOPMODEL were performed by the Shuffled Complex Evolution (SCE-UA) method and evaluated by Kling-Gupta efficiency (KGE) metric. Events 1, 2, and 4 were selected for the calibration stage, with a total duration of 133 days. As for the validation stage, Events 3 and 5 were selected, with a total duration of 156 days. The simulations were performed with a temporal resolution of 24 hours and can be seen in Section 3.2.

3.1. Sensitivity Analysis

The sensitivity of TOPMODEL's parameters can be visually perceived in the parameters that relate the parameter values with the value of the KGE metric. The parameters of soil permeability ($\ln T_e$), decay of transmissivity with depth (m) and average vertical hydraulic conductivity of the surface (k_0), showed significant variations in the simulation results, with both sets of precipitation data (CMORPH and IMERG). **Figure 4** is presented the variations of those parameters' values for the *Chókwè* sub-basin and in **Figure 5** the variations for the *Xai-Xai* sub-basin. The calibrated parameters in each sub-basin are shown in **Table 2**.

Table 2. Calibrated parameters of TOPMODEL for *Chókwè* and *Xai-Xai* with CMORPH and IMERG data sets.

Parameter	*Chókwè*		*Xai-Xai*	
	CMORPH	IMERG	CMORPH	IMERG
$q_{s0}\left[\mathrm{m}\cdot\mathrm{h}^{-1}\right]$	9.52×10^{-3}	1.04×10^{-1}	1.10×10^{-2}	2.78×10^{-2}
$\ln T_e\left[\mathrm{m}^2\cdot\mathrm{h}^{-1}\right]$	7.52×10^{0}	8.37×10^{0}	7.73×10^{0}	8.73×10^{0}
$m\left[\mathrm{m}\right]$	1.26×10^{0}	1.61×10^{0}	1.51×10^{0}	4.22×10^{0}
$S_{r0}\left[\mathrm{m}\right]$	3.54×10^{-7}	7.10×10^{-7}	2.54×10^{-7}	1.21×10^{-7}
$S_{r\max}\left[\mathrm{m}\right]$	1.14×10^{-4}	5.36×10^{-5}	1.15×10^{-4}	5.40×10^{-5}
$t_d\left[\mathrm{h}\cdot\mathrm{m}^{-1}\right]$	1.22×10^{-4}	2.99×10^{-5}	4.02×10^{-5}	3.66×10^{-5}
$v_{CH}\left[\mathrm{m}\cdot\mathrm{h}^{-1}\right]$	2.24×10^{3}	6.84×10^{3}	2.25×10^{3}	2.79×10^{4}
$v_r\left[\mathrm{m}\cdot\mathrm{h}^{-1}\right]$	7.06×10^{4}	1.71×10^{5}	1.42×10^{5}	6.73×10^{4}
$k_0\left[\mathrm{m}\cdot\mathrm{h}^{-1}\right]$	8.36×10^{-1}	3.90×10^{-1}	2.84×10^{0}	2.44×10^{0}
$c_d\left[\mathrm{m}\right]$	6.60×10^{0}	1.47×10^{0}	1.58×10^{0}	4.96×10^{1}

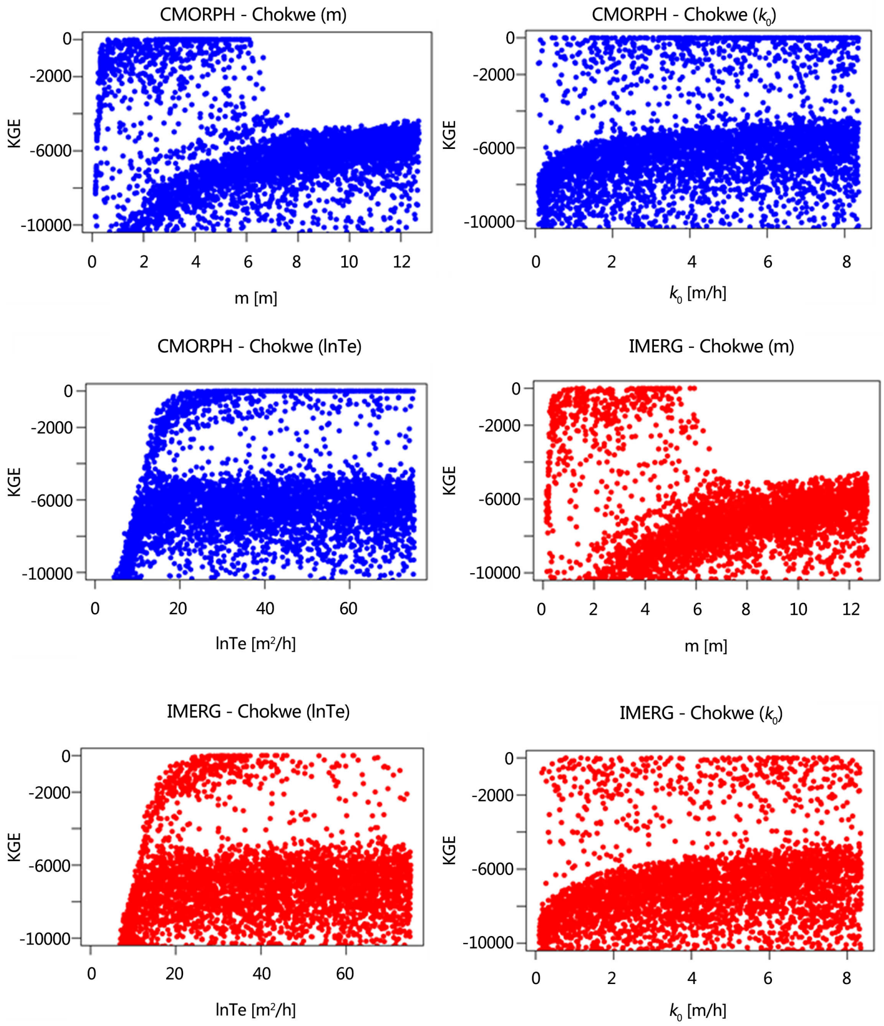

Figure 4. Monte Carlo test of the TOPMODEL parameters that showed sensitivity (m, $\ln T_e$ and k_0) for *Chókwè* with CMORPH (blue) and IMERG (red). Parameter values are shown on the x-axis. Kling-Gupta Efficiency is presented on the y-axis.

According to Hollanda *et al.* (2015) [44], the parameter m is the most important in the TOPMODEL for controlling the hydrological response. Hence, it influences the areas of contribution and the share of precipitation that will become surface runoff. The predominant soils in the Mozambican sub-basins derive from the volcanic sediments of the Karroo, Cretaceous, and Upper Tertiary [10] [11] and are generally constituted by a vast sandy cover of small thickness and a significant amount of clay accumulated in the subsurface layers. These soil characteristics can justify the m values found and their importance in the simulations of flood events.

On the other hand, during the rainy season, the soils of the Mozambican sub-basins remain periodically wet at small depths (from 60 cm), thus having low or very low hydraulic conductivity. This may explain the low values of the parameters $\ln T_e$ and k_0, obtained in the calibration process concerning the values used in the initial estimate of TOPMODEL.

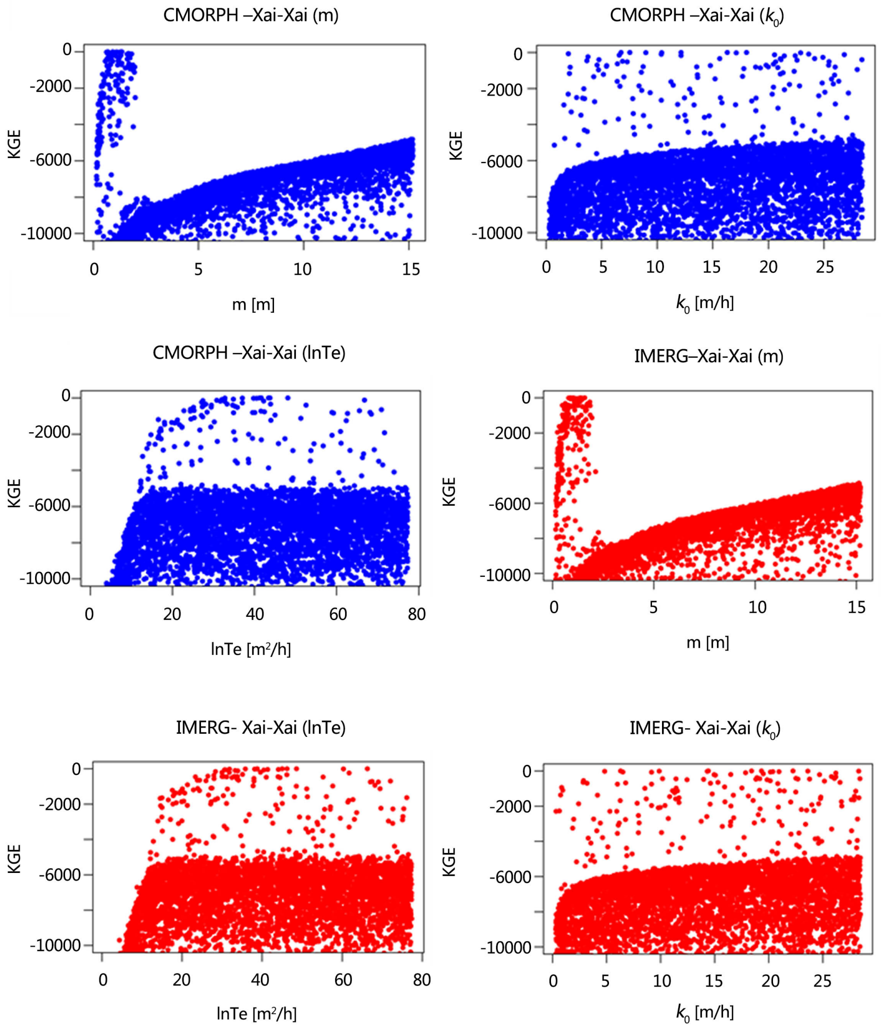

Figure 5. Similar to **Figure 4** except for *Xai-Xai*.

3.2. Simulations

The results of the simulation to flood events for the *Chókwè* subbasin showed that the CMORPH dataset had better performance in the calibration process (KGE = 0.68) about the validation process (KGE = 0.57). Details of these two processes can be seen in **Table 3**. Both datasets showed tendencies to overestimate the stream flows, in most of the maximum peaks of flood events. The peak corresponding to the first 50 days was overestimated (Events 1 and 2) and in x = 110 days (Event 4) was severely underestimated by the IMERG dataset (**Figure 6**). Therefore, during the simulations, the CMORPH dataset presents a similar behavior during the calibration period (**Figure 7**).

For the *Xai-Xai* subbasin, CMORPH and IMERG datasets showed similar behavior, with a good result in the calibration and unsatisfactory in the validation processes (**Table 3**). In the calibration period, the CMORPH dataset obtained better results (KGE = 0.77) compared to IMERG (KGE = 0.65), but the calculated hydrograph presented an amplitude error (overestimated the stream flows) and phase error (delayed and advanced the peak of some events; **Figure 8**). With the IMERG dataset, the simulations presented higher performance in validation processes (KGE = 0.59) in relation to CMORPH (KGE = 0.54). The calculated hydrograph overestimated the stream flows corresponding to Events 1 and 4 (**Figure 9**). This fact may be related to the drainage area of the sub-basin, which is larger than the previous ones (*Chókwè*). Therefore, the performance of TOPMODEL in both regions was good (KGE > 0.5).

Table 3. KGE values for TOPMODEL simulations with CMORPH and IMERG datasets in *Chókwè* and *Xai-Xai* subbasins.

Subbasin	CMORPH		IMERG	
	Calibration	Validation	Calibration	Validation
Chókwè	0.68	0.57	0.62	0.64
Xai-Xai	0.77	0.54	0.65	0.59

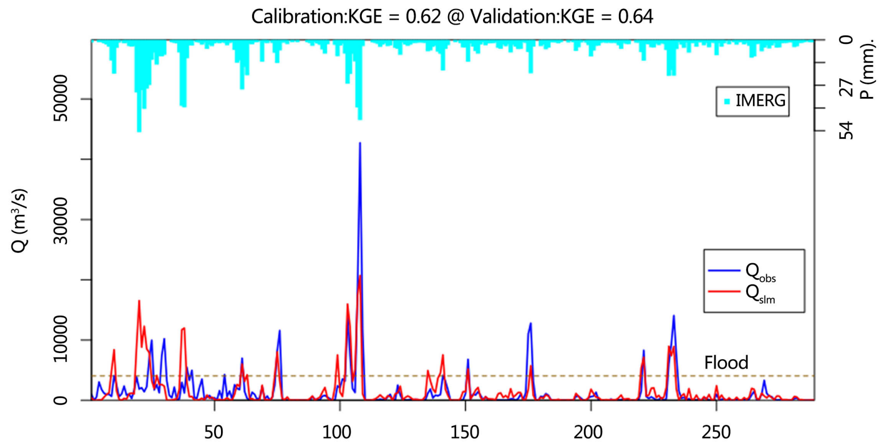

Figure 6. Streamflow ($m^3 \cdot s^{-1}$) time series for Xai-Xai subbasin with IMERG dataset. Observed (blue line) and simulated (red line) data. River stage level thresholds (flood) are indicated by brown dashed lines.

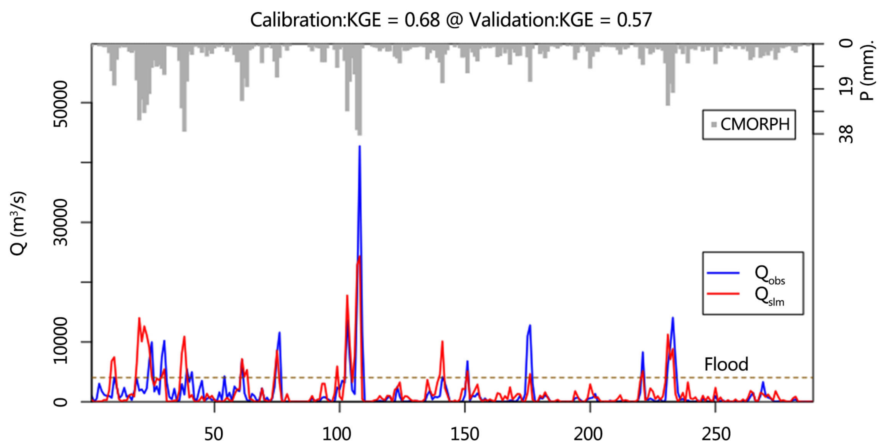

Figure 7. Similar to **Figure 6** except for the CMORPH dataset.

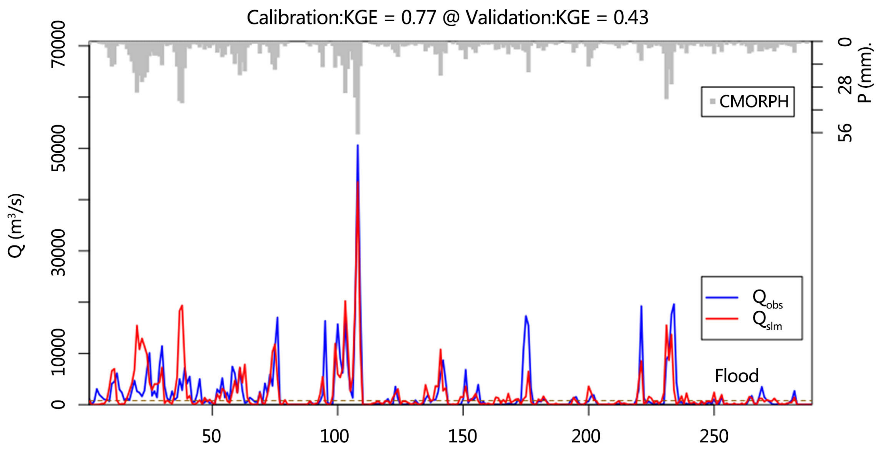

Figure 8. Similar to Figure 6 except for the Xai-Xai subbasin.

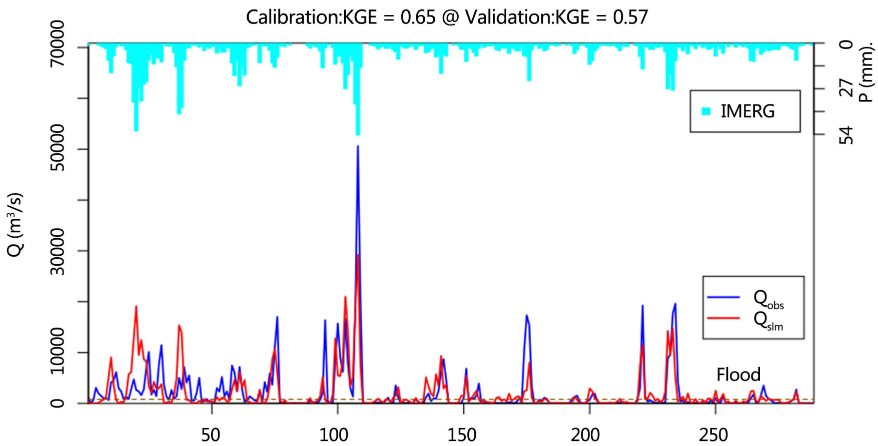

Figure 9. Similar to Figure 6 except for the Xai-Xai subbasin with CMORPH dataset.

4. Conclusions

The main objective of this study was to carry out simulations of flood events that occurred in the *Chókwè* and *Xai-Xai* sub-basins (Mozambican portion of the LRB), between 2000 and 2015 with the TOPMODEL hydrological model using satellite remote sensing data as input. Were used as input data in the model of two satellite-based precipitation estimates products, CMORPH from NOAA and IMERG from NASA. Potential evapotranspiration data from the MOD16 algorithm and surface runoff data from the CLSM/GLDAS model are also used.

Two of the five flood events (Events 1 and 4) described and selected for the simulations with TOPMODEL, were the ones that produced the highest amounts of rain in the LRB region, both with the CMORPH and IMERG datasets. It was 483.6 mm for CMORPH and 550.8 mm for IMERG during Event 1 in 2000. For Event 4, in 2013, the total precipitation amounts were 242.8 mm (CMORPH) and 233.9 mm (IMERG).

To understand the influence of each TOPMODEL parameter in simulations of flood events, sensitivity tests were applied using Monte Carlo Simulations. The parameters that showed significant variations in the simulation results were: m, k_0 and $\ln T_e$. The great sensitivity to the m parameter is mentioned by several authors who performed sensitivity tests with this hydrological model [14] [45] [46] [49] [50]. The parameter k_0, affects both the interflow regime and the flow exchange rate between the unsaturated and saturated zones. During the rainy season, the soils of the Mozambican sub-basins remain periodically wet at small depths, thus having low or very low hydraulic conductivity.

CMORPH showed better performance in the calibration process (0.68 < KGE < 0.77) compared to the IMERG that was better in the validation processes (0.59 < KGE < 0.64). This situation may be related to the physics of rainfall production processes in the region, which can be better detected by the CMORPH algorithm. Overall, the two satellite-based precipitation estimates products show great potential to simulate the streamflow in the LRB region.

Thus, with the results presented in this paper, the TOPMODEL hydrological model can be used in watersheds with similar characteristics in Mozambique; it can also help to develop flood monitoring systems from remotely sensed data; can increase the technical capacity of LRB's water resources managers as well as provide communities with rural areas prior warning of flood events that may occur during the rainy season.

Acknowledgements

The authors are indebted to Mr. Isac Filimone of DNGRH, for providing the hydrometeorological data series used for preliminary analyses. The authors would like to thank CPC/NCEP for providing high-resolution CMORPH datasets, GSFC/NASA for providing GPM-IMERG and surface runoff datasets, LPDAACSVC/USGS for providing potential evapotranspiration data from the MOD16 algorithm. T.E.J. was sponsored by Coordenação de Aperfeiçoamento de Pessoal de Nível Superior (CAPES), and A.J. P.F. by Conselho Nacional de Desenvolvimento Científico e Tecnológico (CNPq) under grant 302349/2017-6.

Conflicts of Interest

The authors declare that they have no known competing financial interests or personal relationships that could have influenced the work reported in this paper.

References

[1] Ingc, U. and Fews, N.M. (2003) Atlas for Disaster Preparedness and Response in the Limpopo Basin. Creda Communications Ltd., Cape Town, 100 p.

[2] Shaviraachin, T. (2005) Flood Simulation: A Case Study in the Lower Limpopo Valley, Mozambique Using the SOBEK Flood Model. Doctoral Thesis, International Institute for Geo-Information Science and Earth Observation, Enschede.

[3] Asante, K.O., Macuacua, R.D., Artan, G.A., Lietzow, R.W. and Verdin, J.P. (2007) Developing a Flood Monitoring System from Remotely Sensed Data for the Limpopo Basin. *IEEE Transactions on Geoscience and Remote Sensing*, **45**, 1709-1714.

https://doi.org/10.1109/TGRS.2006.883147

[4] Asante, K., Brito, R., Brundrit, G., Epstein, P., Nussbaumer, P. and Patt, A. (2009) Study on the Impact of Climate Change on Disaster Risk in Mozambique. INGC Synthesis Report on Climate Change—First Draft, National Institute for Disaster Management, Maputo. http://pure.iiasa.ac.at/9007

[5] Mavume, A.F., Rydberg, L., Rouault, M. and Lutjeharms, J.R. (2009) Climatology and Landfall of Tropical Cyclones in the South-West Indian Ocean. *Western Indian Ocean Journal of Marine Science*, **8**, 15-36. https://doi.org/10.4314/wiojms.v8i1.56672

[6] WMO (2012) Limpopo River Basin: A Proposal to Improve the Flood Forecasting and Early Warning Systems. World Meteorological Organization, Geneva.

[7] Chilundo, M. and Kelderman, P. (2008) Design of a Water Quality Monitoring Network for the Limpopo River Basin in Mozambique. *Physics and Chemistry of the Earth, Parts A/B/C*, **33**, 655-665. https://doi.org/10.1016/j.pce.2008.06.055

[8] Sitoe, S.R., Risberg, J., Norström, E., Snowball, I., Holmgren, K., Achimo, M. and Mugabe, J. (2015) Paleo-Environment and Flooding of the Limpopo River-Plain, Mozambique, between c. AD 1200-2000. *CATENA*, **126**, 105-116. https://doi.org/10.1016/j.catena.2014.10.038

[9] Zhu, T. and Ringler, C. (2012) Climate Change Impacts on Water Availability and Use in the Limpopo River Basin. *Water*, **4**, 63-84. https://doi.org/10.3390/w4010063

[10] Sitoe, S. and Qwist-Hoffman, P. (2013) Limpopo River Basin Monograph. https://dsc.duq.edu/limpopo-policy/1/

[11] Brito, R., Famba, S., Munguambe, P., Ibraimo, N. and Julaia, C. (2009) Profile of the Limpopo Basin in Mozambique. WaterNet Working Paper 11.

[12] Manhique, A.J., Reason, C.J.C., Silinto, B., Zucula, J., Raiva, I., Congolo, F. and Mavume, A.F. (2015) Extreme Rainfall and Floods in Southern Africa in January 2013 and Associated Circulation Patterns. *Natural Hazards*, **77**, 679-691. https://doi.org: 10.1007/s11069-015-1616-y

[13] Rapolaki, R.S., Blamey, R.C., Hermes, J.C. and Reason, C.J.C. (2020) Moisture Sources Associated with Heavy Rainfall over the Limpopo River Basin, Southern Africa. *Climate Dynamics*, **55**, 1473-1487. https://doi.org/10.1007/s00382-020-05336-w

[14] Salviano, M., Pereira Filho, A. and Vemado, F. (2021) TOPMODEL Hydrometeorological Modeling with Rain Gauge Data Integrated by High-Resolution Satellite Estimates. A Case Study in Muriaé River Basin, Brazil. *Atmospheric and Climate Sciences*, **11**, 486-507. https://doi.org/10.4236/acs.2021.113029

[15] Beven, K.J. and Kirkby, M.J. (1979) A Physically Based, Variable Contributing Area Model of Basin Hydrology/Un modèle à base physique de zone d'appel variable de l'hydrologie du bassin versant. *Hydrological Sciences Journal*, **24**, 43-69. https://doi.org/10.1080/02626667909491834

[16] Beven, K.J., Kirkby, M.J., Schofield, N. and Tagg, A.F. (1984) Testing a Physically-Based Flood Forecasting Model (TOPMODEL) for Three UK Catchments. *Journal of Hydrology*, **69**, 119-143. https://doi.org/10.1016/0022-169490159-8

[17] Beven, K. (1997) TOPMODEL: A Critique. *Hydrological Processes*, **11**, 1069-1085. https://doi.org/10.1002/(SICI)1099-1085(199707)11:9<1069::AID-HYP545>3.0.CO;2-O

[18] Beven, K.J. (2012) Rainfall-Runoff Modeling: The Primer. 2nd Edition, John Wiley & Sons, Chichester. https://doi.org/10.1002/9781119951001

[19] Beven, K.J., Kirkby, M.J., Freer, J.E. and Lamb, R. (2021) A History of TOPMODEL. *Hydrology and Earth System Sciences*, **25**, 527-549. https://doi.org/10.5194/hess-25-527-2021

[20] Brock, F.V. and Richardson S.J. (2001) Static Preformance Characteristics, Chapter 3, 46-61.

[21] Alsumaiti, T.S., Hussein, K., Ghebreyesus, D.T. and Sharif, H.O. (2020) Performance of the CMORPH and GPM IMERG Products over the United Arab Emirates. *Remote Sensing*, **12**, Article No. 1426. https://doi.org/10.3390/rs12091426

[22] Joyce, R.J., Janowiak, J.E., Arkin, P.A. and Xie, P. (2004) CMORPH: A Method that Produces Global Precipitation Estimates from Passive Microwave and Infrared Data at High Spatial and Temporal Resolution. *Journal of Hydrometeorology*, **5**, 487-503. https://doi.org/10.1175/1525-7541(2004)005<0487:CAMTPG>2.0.CO;2

[23] Huffman, G.J., Bolvin, D.T., Braithwaite, D., Hsu, K.L., Joyce, R.J., Kidd, C., *et al.* (2019). Integrated Multi-Satellite Retrievals for the Global Precipitation Measurement (GPM) Mission (IMERG). In: Levizzani, V., Kidd, C., Kirschbaum, D.B., Kummerow, C.D., Nakamura, K. and Turk, F.J., Eds., *Satellite Precipitation Measurement*, Springer, Cham, 343-353. https://doi.org/10.1007/978-3-030-24568-9_19

[24] Mu, Q., Zhao, M. and Running, S.W. (2011) Improvements to a MODIS Global Terrestrial Evapotranspiration Algorithm. *Remote Sensing of Environment*, **115**, 1781-1800. https://doi.org/10.1016/j.rse.2011.02.019

[25] Rodell, M., Houser, P.R., Jambor, U.E.A., Gottschalck, J., Mitchell, K., Meng, C.J., *et al.* (2004) The Global Land Data Assimilation System. *Bulletin of the American Meteorological Society*, **85**, 381-394. https://doi.org/10.1175/BAMS-85-3-381

[26] Duan, Q., Sorooshian, S. and Gupta, V. (1992) Effective and Efficient Global Optimization for Conceptual Rainfall-Runoff Models. *Water Resources Research*, **28**, 1015-1031. https://doi.org/10.1029/91WR02985

[27] Naeini, M.R., Analui, B., Gupta, H.V., Duan, Q. and Sorooshian, S. (2019) Three Decades of the Shuffled Complex Evolution (SCE-UA) Optimization Algorithm: Review and Applications. *Scientia Iranica*, **26**, 2015-2031.

[28] Nash, J.E. and Sutcliffe, J.V. (1970) River Flow Forecasting through Conceptual Models Part I—A Discussion of Principles. *Journal of Hydrology*, **10**, 282-290. https://doi.org/10.1016/0022-169490255-6

[29] Gupta, H.V., Kling, H., Yilmaz, K.K. and Martinez, G.F. (2009) Decomposition of the Mean Squared Error and NSE Performance Criteria: Implications for Improving Hydrological Modeling. *Journal of Hydrology*, **377**, 80-91. https://doi.org/10.1016/j.jhydrol.2009.08.003

[30] Knoben, W.J., Freer, J.E. and Woods, R.A. (2019) Inherent Benchmark or Not? Comparing Nash-Sutcliffe, and Kling-Gupta Efficiency Scores. *Hydrology and Earth System Sciences*, **23**, 4323-4331. https://doi.org/10.5194/hess-23-4323-2019

[31] Duan, Q., Sorooshian, S. and Gupta, V.K. (1994) Optimal Use of the SCE-UA Global Optimization Method for Calibrating Watershed Models. *Journal of Hydrology*, **158**, 265-284. https://doi.org/10.1016/0022-169490057-4

[32] Franchini, M., Wendling, J., Obled, C. and Todini, E. (1996) Physical Interpretation and Sensitivity Analysis of the TOPMODEL. *Journal of Hydrology*, **175**, 293-338. https://doi.org/10.1016/S0022-169480015-1

[33] Tucci, C.E.M. (1998) Modelos hidrológicos. Universidade Federal do Rio Grande do Sul, Porto Alegre.

[34] Brighenti, T.M., Bonumá, N.B., Chaffe, P.L.B., Grison, F. and Kobiyama, M. (2017) Análise de sensibilidade como primeiro passo para modelagem hidrológica: Estudo

de caso do o modelo SWAT. *Simpósio Brasileiro de Recursos Hídricos*, Porto Alegre, 26 November-1 December 2017, 8 p.. https://anais.abrhidro.org.br/job.php?Job=2479

[35] Reason, C.J. and Smart, S. (2015) Tropical Southeast Atlantic Warm Events and Associated Rainfall Anomalies over Southern Africa. *Frontiers in Environmental Science*, **3**, Article No. 24. https://doi.org/10.3389/fenvs.2015.00024

[36] Kidd, C. and Huffman, G. (2011) Global Precipitation Measurement. *Meteorological Applications*, **18**, 334-353. https://doi.org/10.1002/met.284

[37] Joyce, R.J., Xie, P., Yarosh, Y., Janowiak, J.E. and Arkin, P.A. (2010) CMORPH: A "Morphing" Approach for High-Resolution Precipitation Product Generation. In: Gebremichael, M. and Hossain, F., Eds., *Satellite Rainfall Applications for Surface Hydrology*, Springer, Dordrecht, 23-37. https://doi.org/10.1007/978-90-481-2915-7_2

[38] Pereira Filho, A.J., Vemado, F., Vemado, G., Gomes Vieira Reis, F.A., Giordano, L.D.C., Cerri, R.I., *et al.* (2018) A Step towards Integrating CMORPH Precipitation Estimation with Rain Gauge Measurements. *Advances in Meteorology*, **2018**, Article ID: 2095304. https://doi.org/10.1155/2018/2095304

[39] Janowiak, J.E., Kousky, V.E. and Joyce, R.J. (2005) Diurnal Cycle of Precipitation Determined from the CMORPH High Spatial and Temporal Resolution Global Precipitation Analyses. *Journal of Geophysical Research*: *Atmospheres*, **110**, Article ID: D23105. https://doi.org/10.1029/2005JD006156

[40] Monteith, J.L. (1965) Evaporation and Environment. *Symposia of the Society for Experimental Biology*, **19**, 205-234.

[41] Ruhoff, A.L., Aragão, L.E.O., Collischonn, W., Rocha, H.R.D., Mu, Q. and Running, S. (2011) MOD16: Desafios e limitações para a estimativa global de evapotranspiração. Repositório Institucional (RI) da Universidade Federal do Rio Grande do Sul (UFRGS), http://repositorio.furg.br/handle/1/1256

[42] Running, S., Mu, Q., Zhao, M. and Moreno, A. (2019) MOD16A2GF MODIS/Terra Net Evapotranspiration Gap-Filled 8-Day L4 Global 500 m SIN Grid V006 [Data set]. NASA EOSDIS Land Processes DAAC.

[43] Silva, F.B. (2013) Modelagem da produtividade primária bruta na Amazônia. Tese de Doutorado em Sensoriamento Remoto-Instituto Nacional de Pesquisas Espaciais. São José dos Campos, São Paulo.

[44] Hollanda, M.P., Cecilio, R.A., Campanharo, W.A., Zanetti, S.S., de Andrade, L.N. and Garcia, G.D.O. (2015) Evaluation of TOPMODEL for Prediction of the Runoff of a Watershed under Different Land Uses/Avaliação do TOPMODEL na estimativa do escoamento superficial em microbacia hidrográfica em diferentes usos. *Revista Brasileira de Engenharia Agrícola e Ambiental*, **19**, 489-497. https://doi.org/10.1590/1807-1929/agriambi.v19n5p489-496 https://www.scielo.br/j/rbeaa/a/cyB8frq8dfnTJKSrkH4SMwJ/?lang=pt

[45] Muhammed, A.H. (2012) Satellite-Based Evapotranspiration Estimation and Runoff Simulation: A Topmodel Application to the Gilgel Abay Catchment, Ethiopia. Master's Thesis, University of Twente, Enschede.

[46] Schuler, A.E., Moraes, J.D., Milde, L.C., Groppo, J.D., Martinelli, L.A., Victoria, R.L. and Calijuri, M.L. (2000) Análise da representatividade física dos parâmetros do TOPMODEL em uma bacia de mesoescala localizada nas cabeceiras do Rio Corumbataí, São Paulo. *Revista Brasileira de Recursos Hídricos*, **5**, 5-25.

[47] Campling, P., Gobin, A., Beven, K. and Feyen, J. (2002) Rainfall-Runoff Modeling of a Humid Tropical Catchment: The TOPMODEL Approach. *Hydrological Processes*,

16, 231-253. https://doi.org/10.1002/hyp.341

[48] Van Zyl, J.J. (2001) The Shuttle Radar Topography Mission (SRTM): A Breakthrough in Remote Sensing of Topography. *Acta Astronautica*, **48**, 559-565. https://doi.org/10.1016/S0094-576500020-0

[49] Silva, R.D. and Kobiyama, M. (2007) Estudo comparativo de três formulações do TOPMODEL na bacia do Rio Pequeno, São José dos Pinhais, PR. *Revista Brasileira de Recursos Hídricos*, **12**, 93-105.

[50] Rocha Filho, K.L.D. (2010) Modelagem Hidrológica da Bacia do Rio Pirajuçara com TOPMODEL, Telemetria e Radar Meteorológico. Master Dissertation, Universidade de São Paulo, São Paulo.